

## DAMAGE CHARACTERIZATION OF AEROSPACE CFRP PANELS AFTER IMPACT TESTING

N. Gutiérrez<sup>a\*</sup>, R. Fernández<sup>a</sup>, M.L. Santamaría<sup>a</sup>, C. Galleguillos<sup>a</sup>, G. Morales<sup>b</sup>, F. Lasagni<sup>a</sup>

<sup>a</sup>Materials & Processes dept., Center for Advanced Aerospace Technologies - CATEC, C/Wilbur y Orville Wright, 17-19-21, 41309 La Rinconada (Sevilla), Spain

<sup>b</sup>R&D-Technology Department, Alestis Aerospace, C/ De los Hnos. d'Eluyar s/n, 41092. Isla de la Cartuja, Sevilla, Spain

\*ngutierrez@catec.aero

**Keywords:** Impact damage, CFRP, Tomography, Ultrasonics.

### Abstract:

*Polymer matrix composite materials have played a major role for weight reduction of aerospace structures. Particularly, continuous Carbon Fiber Reinforced Polymers (CFRPs) are extremely strong with a remarkable fatigue behavior. On the other hand, these materials present usually poor impact damage tolerance.*

*In this work, the impact behavior of CFRP materials manufactured by pre-preg lamination and autoclave curing is analyzed. A non-destructive evaluation of test specimens is performed prior and after low energy impact testing. X-Ray tomographic analyses are also carried out for three dimensional characterization of damage, and correlation studies of the impact energy and affected areas of the test elements.*

### 1. Introduction

CFRP materials have become more and more familiar for many uses and industries. Transport sectors like automotive and especially aerospace are increasing their content in their late products. Composite is normally a synonym of quality, high performance, low weight and innovation. During the last four decades, reinforced plastics have inherited these qualifying due to their specific high stiffness (young modulus), ultimate strength, elastic behavior, corrosion resistance properties, between many others. One of the drawbacks of this family of materials is damage tolerance and its detection. Composite absorbs energy in form of internal damage mechanisms like delamination, fiber breakage, fiber-matrix interface debondings.... Low speed impacts, commonly produced during manufacturing or handling, promotes these types of failure [1,2]. Damages can reduce ultimate strength up to a 60% [3-6].

Due to their internal mechanism of damaged development, external signs are not easy to neither detect nor quantify. Typically, damage evaluation after impact events is performed by means of ultrasonic (UT) inspections. UT Phase Array (PA) allows a fast inspection of CFRP laminates, and the generation of three-dimensional (3D) cartographies. From these, the extension and depth of the damage can be calculated. X-ray Computed Tomography (CT) has gain more importance as characterization technique in the last decades. It consists of making

hundreds of X-ray projections of the test element over a digital detector and combining all of them to reconstruct it in a 3D virtual representation. Detailed information for damage characterization can be obtained, dealing into accurate representation of the associated defectology (like delaminations, fiber-matrix interface debondings, fiber breakage, ...).

A non-destructive evaluation of impacted pre-preg/cured laminates is performed in this work. Specimens were analyzed after low-medium energy impacts by ultrasonics PA and computed tomography. Dimensional relationships are obtained between the analyzed features and against the absorbed energy during an impact event.

## 2. Methodology

### 2.1. Materials

Six samples were extracted from two different CFRP panels (identified as A and B) have been investigated, with dimensions of 100x150 mm and 1.5 mm thickness. Panels were manufactured from 7 layers of unidirectional prepreg with the next lamination order (45/-45/90/0)<sub>s</sub> and then cured in autoclave.

### 2.2. Equipment

Ultrasonic PA inspections were performed by using an Olympus Omniscan MX16:128, a probe phased array and 5MHz@64 elements phased array probe. Linear encoder (mini-wheel) has been employed for the register of signal position. Testing parameters are presented in Table 1.

Parameter	Value
Gain (dB)	0.5-2.5
Speed (m/s)	3015.9
Sum Gain (dB)	10

**Table 1.** US-PA inspection parameters for sample inspections.

Impact tests were carried out by means of an impact tower Ceast 9350 (Instron) and a digital acquisition system DAS 16000. Impacts were performed through a hemispherical impactor of 10 mm in diameter and a mass of 2.048 kg. Impact energies were selected at 4, 7 and 10 J (Table 2). All tests were performed at room temperature.

Specimen ID	Impact Energy [J]
A-1	4
A-2	7
A-3	10
B-1	4
B-2	7
B-3	10

**Table 2.** CFRP Specimens and energies for impact testing.

An X-ray computed tomography system VJT-225  $\mu$ -CT / VJ Technologies was used for three dimensional investigations. VGStudio software was selected for data reconstruction. Testing parameters are presented in Table 3.

Parameters	Value
Voltage (kV)	100
Amperage ( $\mu$ A)	200
Nr. of projections	800
Average Images	4
Skip Image	1
Voxel resolution [ $\mu$ m]	40

**Table 3.** CT inspection parameters.

Image J software (open source, Java-based program developed at the National Institute of Health in the USA [7]) was used for processing the obtained cross-sections. It provides extensibility via Java plugins and recordable macros. Custom acquisition, analysis, filtering and processing plugins can be developed using built-in editor and a Java compiler.

### 2.3. Testing methodology

First, the two CFRP panels were inspected by US PA in order to detect any possible flaw introduced during manufacturing. No irregularity was discovered. After that, 3 samples for each panel (A-1, 2 and 3, & B-1, 2 and 3) were prepared.

Impacts were performed from low to high energies. Damage depth was recorder with a calibrated caliper after impact. Energy vs. time charts were obtained during impact testing, allowing the quantification of energy absorption. After that, US inspections were developed with same configuration parameters over the impacted face. In this way, area of damage was calculated through the obtained C-scans in amplitude and position. Once all information collected, Image J was used to estimate affected area.

Finally, tomographic analysis was performed on impacted specimens. Precise dimensioning of damage volume was performed. Cracks and delaminations on impacted area were characterized as well.

## 3. Results

Figure 2 shows C-scans in (a) amplitude and in (b) position of specimen B-3 after 10J impact. The affected area was quantified in 2,212.294 mm<sup>2</sup> in the C-Scan. Similarly, the affected area

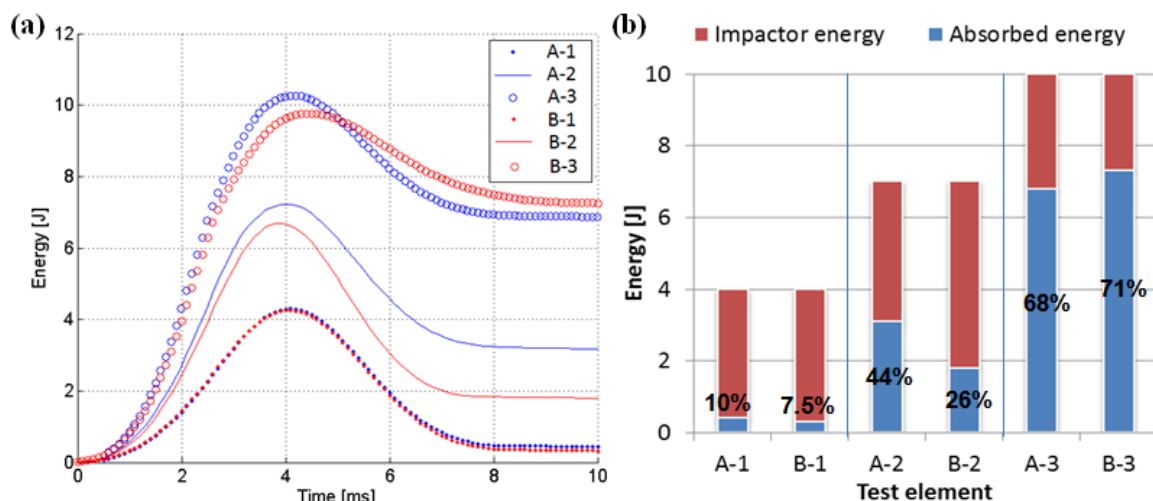


**Figure 1.** (a) Energy vs. time graph; and (b) absorbed vs. impact energy ratio (b).

after impact event for all test specimens are presented in Table 4. A huge variation in the damage area is recorded, averaging 276 mm<sup>2</sup> after 4J impact, to more than 2,000 mm<sup>2</sup> after 10J event (~ 7.6 times larger).

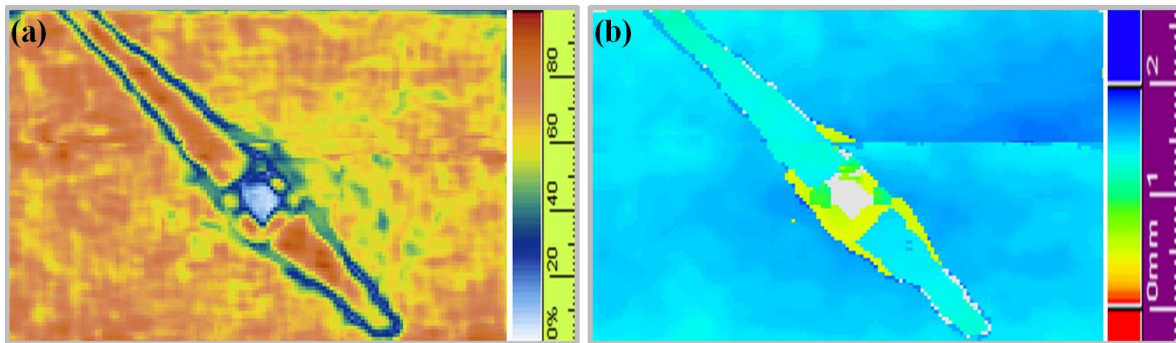


Figure 2. C-scan in (a) amplitude and (b) position for B-3.

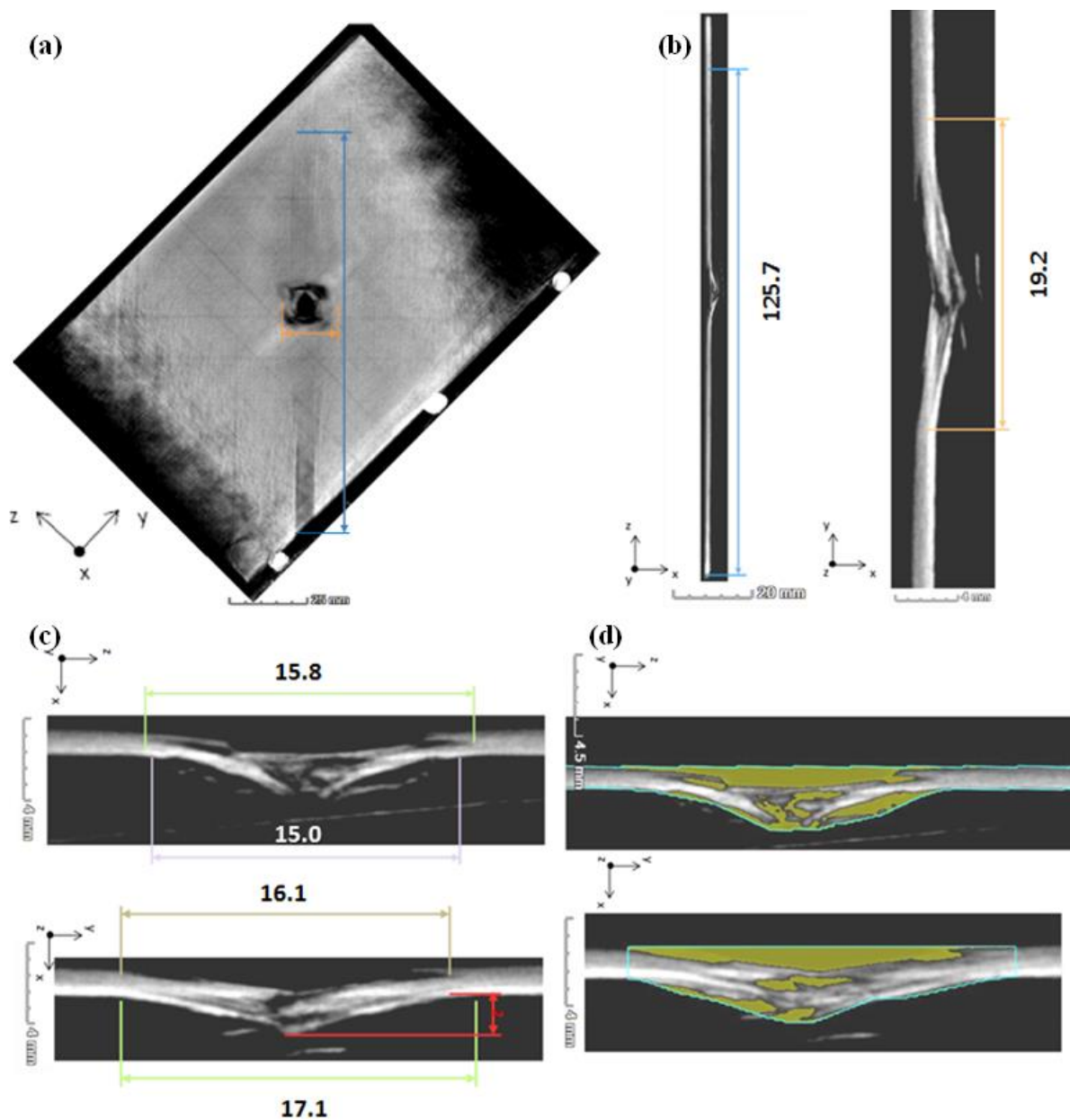


Figure 3. Tomographic cross sections for sample B-3: (a) top and (b) lateral views at impact damage locations; dimensioning of damage area (c) 2D measures and (d) volume calculation.

Tomographic cross sections of the delaminated volume is depicted in Figure 3 for sample B-3. Fiber and matrix breakage is clearly observable, showing conical shape. A surface area of 15 to 19 mm in diameter is affected by the impactor. Fiber are spread 2 mm from the back face. The recorded longitudinal delamination extends up to 125.7 mm along the sample. Volume of damage area is calculated from 3D views. An example for volume quantification process is depicted in Fig. 3d, amounting almost 190 mm<sup>3</sup> after 10J impact. This value shows much lower in specimens impacted with total energy of 4J (-65%) and ranging between 32-100mm<sup>3</sup> (-35%) after 7J impacts. High variation of the recorded volume is observed for samples A-3 (impacted at 10J), showing a damage region of 776.7 mm<sup>3</sup>. This is mainly due to the appearance of large delamination along the whole specimen.

Sample ID	Impacted Energy (IE) [J]	Absorbed Energy [J] (% of IE)	Dent depth [mm]	Affected area [mm <sup>2</sup> ]	Affect. Vol. [mm <sup>3</sup> ]
A-1	4	0.4 (10%)	0.08	276.4	11.81
A-2	7	3.1 (44%)	0.45	770.4	99.6
A-3	10	6.8 (68%)	1.13	1,975.7	776.7(*)
B-1	4	0.3 (7.5%)	0.06	263.6	12.1
B-2	7	1.8 (26%)	0.25	423.7	32
B-3	10	7.3 (73%)	1.2	2,212.3	188.7

**Table 4.** Impact and absorbed energy, dent depth, area and volume affected for all specimens.

(\*) This measure is remarkably high due to quantification of volume under a spread fiber.

The summarized results by the different characterization methods are presented in Table 4. Several relationships can be obtained:

(i) There is a clear correlation between the absorbed energy and microstructural analyzed features (Figure 4). Regression coefficients  $R^2$  larger than 0.98 are recorded after linear regression of relationships absorbed energy vs. dent depth (measured by caliper), damage area (ultrasonic) and volume (tomography).

(ii) A linear relation is also obtained between the analyzed features. Regression coefficients larger than 0.95 are calculated for the relationships dent depth vs. area and volume (Figure 5). This is related with the conical shape observed for the analyzed damage in the laminates.

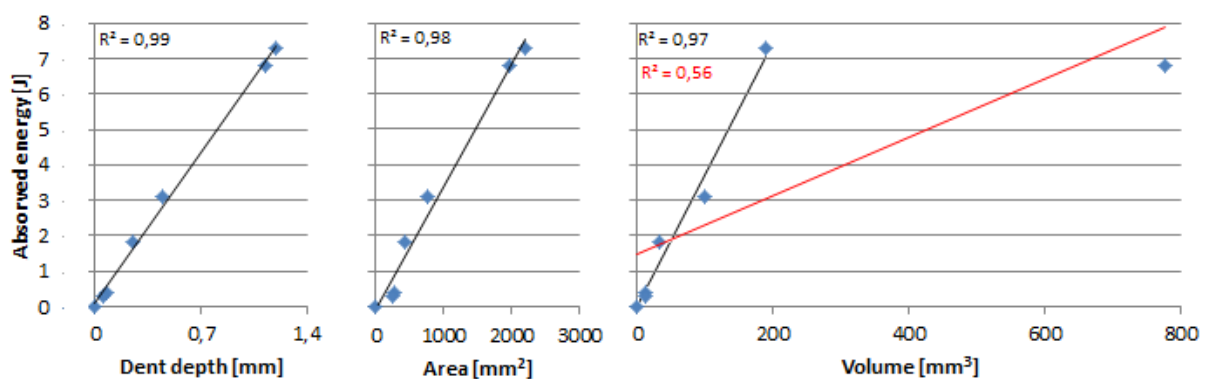


**Figure 4.** Relationship graphs of absorbed energy vs dent depth, affected area and volume for all specimens. Regression lines are also depicted in black, in red with A-3 (Volume only).

It must be noticed that for the case of specimen A-3, the quantification in volume of damage is critically increased due to the apparition of an out-of plane delamination (see Figure 6).

Therefore, a strong variation in the linearity ( $R^2 < 0.58$ ) for volumetric comparisons is recorded.

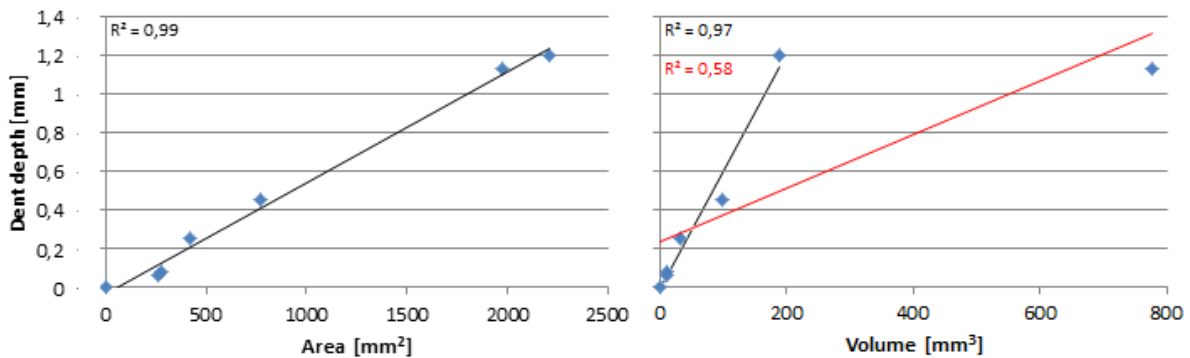


**Figure 5.** Relationship graphs of dent depth vs. affected area and volume for all specimens. Regression lines are also depicted in black, in red with A-3 (Volume only).

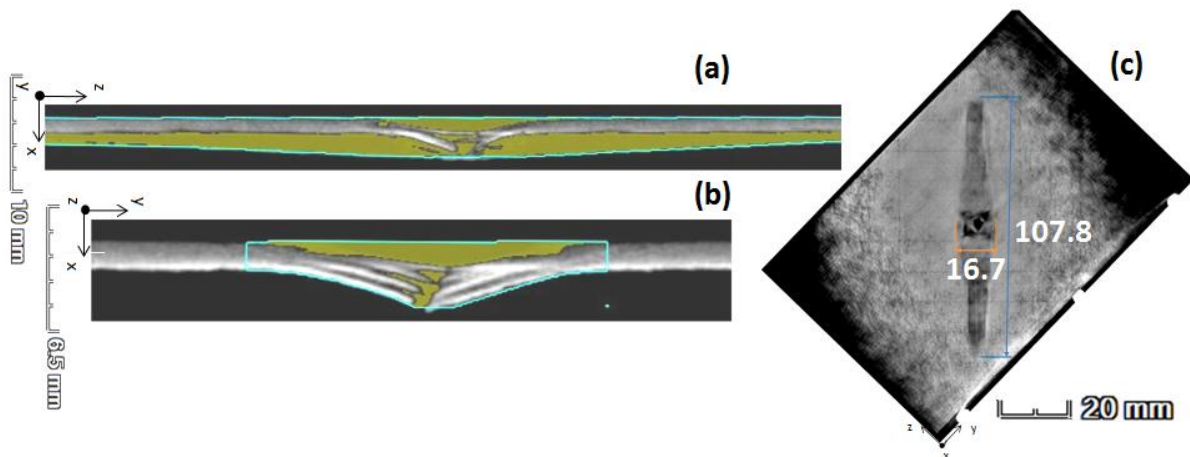


**Figure 6.** Tomographic cross sections for sample A-3: (a) and (b) volume calculation, (c) top view at impact damage location.

#### 4. Conclusions

Only up to 10% of the energy is absorbed by the laminates at low impact energies (4J), where damage lower than 12 mm<sup>3</sup> are recorded after tomographic analysis. This value represents only about 6% of the accumulated damage after 10J impacts (2.5 times larger than low energy impacts). During high energy impacts (10J) the absorbed energy increases up to 70%, dealing in much larger damages.

There is a good relation between the analyzed microstructural features for damage characterization. A linear regression can be simply estimated for recording the progress of damage (by means of the dent depth, affected area or volume) against the absorbed energy. Since most of the damages analyzed in this work correspond to classical conical shape, the three analyzed features are related by a linear relation.

Although, ultrasonic C-scans provide an accurate estimation of the recorded damages, only X-ray tomography allows their volumetric 3D characterization and quantification of the whole affected region. Due to the physics of the method, ultrasonics technique is not capable of characterizing the superposed delaminations that typically appear during an impact event.

## References

- [1] M.J. Santos, J.B. Santos, A.M. Amaro, M.A. Neto. Low velocity impact damage evaluation in plates using PZT sensors. *Composites: Part B* 55, 269-276,2013.
- [2] Collombet F, Bonini J, Lataillade JL. A three-dimensional modelling of low velocity impact damage in composite laminates. *Int J Numer Meth Eng* 39, 1491-516.1996
- [3] Amaro AM, Reis PNB, Moura MFSF, Santos JB. Damage Detection on laminated composite materials using several NDT techniques. *Insight* 54,14-20,2012.
- [4] Abrate S. Impact on laminated composite materials. *Appl Mech* 44,55-91,Rev 1991.
- [5] Cantwell WJ, Morton J. Comparison of the low and high velocity impact response of CFRP. *Composites* 20,545-51,1989.
- [6] de Moura MF, Marques AT. Prediction of low velocity impact damage in carbon-epoxy laminates. *Compos Part A: Appl S* 2002,33,361-8.
- [7] Schneider CA, Rasband WS, Eliceiri KW. NIH Image to ImageJ: 25 years of image analysis. *Nat Methods* 9 (7): 671–675. 2012.